Smooth Non Linear High Gain Observers for a Class of Dynamical Systems

JOSÉ ANTONIO GONZÁLEZ-PRIETO[1] **AND ALEJANDRO F. VILLAVERDE**[2]

[1]Centro Universitario de la Defensa, Escuela Naval Militar, Marín, 36920 Galicia, Spain
[2]Department of Systems Engineering and Control, Universidade de Vigo, Vigo, 36310 Galicia, Spain

Corresponding author: José Antonio González-Prieto (jose.gonzalez@cud.uvigo.es)

ABSTRACT High-gain observers are powerful tools for estimating the state of nonlinear systems. However, their design poses several challenges due to the need of dealing with phenomena such as peaking and chattering. To address these issues, we propose a differentiator operator design based on a non linear second order high-gain observer, which is suited to a class of dynamical systems. Our method includes a procedure to determine high gains in order to avoid chattering in the case of noise-free models, and cut-off frequency based gain design in the case of noisy measurements. Complementary, we suggest performing observability analyses to ensure *a priori* the feasibility of the estimation. The main strengths of our approach are its simplicity and robustness. We demonstrate the performance of the proposed method by applying it to two processes (chemical and biological).

INDEX TERMS Biosystems, chattering phenomenon, high gain observers, observability, peaking phenomenon, process control, state estimation.

I. INTRODUCTION

The observation and estimation of unmeasured system states and unknown parameters of a dynamical system is an important problem in process control. As discussed in [1], at least two distinct approaches to this problem can be found in the literature: estimation with differentiator techniques [2]–[6] and estimation with dynamical observers. Work on this topic focused initially on linear systems [7], [8], and was later extended to nonlinear systems using approaches such as linearisation assumptions on the structure of the dynamics [9]–[11], multivariable circle criterion [12], sliding mode approaches [13]–[21], and high-gain observers [22]–[36]. The application of observers to chemical processes has been reviewed in [37], with examples of design including [38]–[45].

High-gain observers, which have excellent robustness properties, have been developed for systems that can be transformed into one of the available normal forms. This methodology guarantees the existence of an exponentially

convergent observer; it has only one tuning parameter, which should be set to a sufficiently large value.

Assuming that there is no noise, by setting the observer gain to a sufficiently large value the observer error can be made arbitrarily small. However, choosing an adequate value can be challenging in practical applications, mainly due to two issues: the peaking and chattering phenomena.

The *peaking phenomenon* occurs when high-gain feedback leads certain states to very large values before they rapidly decay to zero. These states may destabilize the system, and even make certain states reach infinite values in finite escape time [46]. To understand this phenomenon, consider the problem of differentiating a state x_1 subject to unknown inputs that affect its derivative. At the beginning of the observation process, the first variable of the observer, z_1, converges rapidly with respect to the system dynamics, until the estimation error $e = x_1 - z_1$ reaches zero. During this reaching phase, the derivative estimated by the second observer state, $z_2 = \dot{z}_1$, reaches high values due to the fast convergence of z_1, causing a narrow large peak in the initial estimation $x_2 = \hat{\dot{x}}_1$. Since the observer is much faster than the observed system, the peaking period is very short relative to the time scale of the closed-loop dynamics, hence appearing in the transitory response.

The *chattering phenomenon* is difficult to define mathematically; it consists of high-frequency, finite-amplitude oscillations [47]. Two possible sources are: the use of non-continuous functions (such us the set valued sign function used in classical sliding mode control), and discretization (which can introduce chattering in the steady-state response if the gains are large enough, even if all the functions are continuous, as long as the system dynamics includes high frequency components with respect to the sampling time τ).

Another issue that might impact the upper bounds for high gain observers is the presence of noise in output signals, to which the observer may be highly sensitive [27], specially to output measurement noise for higher dimensional systems having nonlinearities with large *Lipschitz* constant. This problem can be tackled using time-varying gains, switched approaches, or low-pass filters, in order to attenuate noise sensitivity [5].

It is worth mentioning that the theoretical possibility of inferring the state of a system from the observations of the output (i.e. the *observability* problem) should also be taken into account. This property must be assessed *a priori* to guarantee that the state estimation is feasible, thus ruling out the existence of estimation artifacts. The observability of nonlinear systems can be analysed with differential geometric techniques [48], which are available in state of the art tools. This is the approach that we adopt in the present work. It is also important to consider the *implementation aspects* of the observer design. Numerical computations can be problematic in practice, especially when the dimension of the observer is high. To this end, cascade connections [30], [34], [49] have been proposed to reduce computational complexity. Besides, a graphical approach can be used to guide the cascade observer design. By describing the dynamical system of interest as a network, paths in the corresponding structural graph determine the cascade operations that solve the observation problem. In this context, a solution to the observation design problem can be seen as a logical sequence of operations between nodes that create a path along the graph [50]–[53].

In said graphs each node represents a state, and an edge indicates that a state is present at the differential equation of other state. Linear and nonlinear relations are represented by continuous and dashed edges, respectively. The observability of nonlinear systems may depend on the trajectory, because nonlinear connections can vanish at some regions of the state space. In this work we propose a graphical representation of the dynamical system that includes its states and functions, and we use two types of operators (differentiation and inversion) to create solution paths in the graph. Applying these two operators we show how to tune them to avoid chattering. Our differentiator includes linear and nonlinear functions tuned to avoid peaking and chattering.

We implement the methodology in MATLAB and we demonstrate its performance with analytic results and numerical simulations of two case studies, considering both noise-free and noisy scenarios.

Thus, the integrated approach proposed in this paper addresses five aforementioned aspects of observer design: peaking, chattering, noisy measurements, numerical implementation and observability analysis.

The paper is organized as follows. First, in Section II we present the class of dynamical problems that are suitable for the method, and we present a functional graph based on its structure, consisting of a sequence of two operators – differentiation and inversion – that solve the observation problem. Then, in Section III we show how to design the differentiator operator based on a non linear second order high-gain observer, which we refer to as the Smooth Nonlinear Super-Twisting Approximation (SNSTA). In Section IV we describe the semi-implicit discretization of the continuous algorithm and determine its parameters, i.e. the gains accounting for the chattering phenomenon. We discuss observability analysis in Section V. We demonstrate the proposed approach with two case studies in Section VI. Finally, we summarize the conclusions and discuss future developments in Section VII.

II. PROBLEM STATEMENT AND PROPOSED SEQUENCE OF OPERATORS
A. DYNAMICAL SYSTEMS STUDIED IN THIS WORK
In this work we consider the following class of nonlinear dynamical systems, which is a generalization of the classic triangular normal form

$$
\begin{aligned}
\dot{x}_1(t) &= f_1([x_1, u], x_2) + g_1([x_1, u]) \\
\dot{x}_2(t) &= f_2([x_1, x_2, u], x_3) + g_2([x_1, x_2, u]) \\
\dot{x}_3(t) &= f_3([x_1, x_2, x_3, u]) \\
y(t) &= x_1(t) + n(t)
\end{aligned}
\tag{1}
$$

where the notation $[x]$ denotes that the presence of the variable in the function is optional. In this model $x_1(t)$ is the measurable state, $x_2(t)$ and $x_3(t)$ are non measurable states, $u(t)$ is the input excitation, usually a control input signal and $n(t)$ is the noise that corrupts the measured state. To present the results clearly, we exclude from the notation the temporal dependence of the state variables and the state dependency of the model functions.

It is assumed that f_2, g_2, f_1 and g_1 are sufficiently smooth functions with known expressions, and f_3 is an unknown function. Note that, since f_3 is unknown, it allows for the possibility of rewriting systems of dimension higher than three in the above form, thus providing additional flexibility. If f_3 is known, an additional state or parameter may be estimated, as will be shown in the numerical simulations.

The class of nonlinear dynamical systems (1) can be used to describe, among others, chemical and biological processes such as the case studies presented in Section VI, including processes with up to three states, in which it is often the case that only one output can be measured. This class includes some systems that cannot be modeled with the classic triangular normal form, as e.g. the continuous stirred-tank reactor
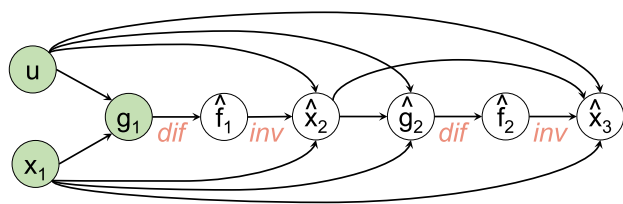
FIGURE 1. Observation graph: logical sequence of operators that solves the observation problem. Green shaded circles denote known variables (u, x_1) and the function that can be directly computed from them (g_1). Estimated variables and functions are displayed in white with a hat ($\hat{*}$). The differentiator and inversion operators are denoted as *dif* and *inv*.

considered in Section VI. More complex dynamical systems can arise as networks of interconnected models of this class.

The observability of system (1) depends on the expressions of its functions, that is, on the properties of the maps between model variables defined by f_i and g_i.

B. A LOGICAL SEQUENCE OF OPERATORS THAT SOLVES THE OBSERVATION PROBLEM

The objective is to estimate the values of the hidden states $x_2(t)$ and $x_3(t)$ by means of the knowledge of the expressions of f_2, g_2, f_1, and g_1, the system input $u(t)$, and the measured state $x_1(t)$, under some assumptions. To this end we present an algorithmic procedure consisting of a logical sequence, which we obtain from the graph shown in Figure 1. In this graph, the operators used to solve the problem are:

- $f(x) \xrightarrow[x(t)]{\text{dif}} \hat{d}(t)$: This operator represents the use of a differentiator to estimate the unknown term $d(t)$ in the following differential equation,

$$\dot{x}(t) = f(x) + d(t),$$

  by means of the available information, $x(t)$ and $f(x)$. As commented in [27], a high-gain observer provides a solution to obtain a fast and robust estimation $\hat{d}(t) \approx d(t)$.

- $h \xrightarrow[x(t)]{\text{inv}} y(t)$: In this case we assume that in a function $h(x, y)$ it is possible to calculate $y(t)$ from the values of $h(x, y)$ and $x(t)$. From the implicit function theorem, this condition is achieved on a domain X of x if $\frac{\partial f}{\partial y} \neq 0 \ \forall x \in X$. The domain X determines the state space region where the proposed solution can be applied.

The restrictions that must be considered in order to apply the proposed operators are:

- $\frac{\partial f_1}{\partial x_2} \neq 0 \ \forall([x_1, u])$, so that it is possible to apply the operator:

$$f_1 \xrightarrow[{[x_1, u]}]{\text{inv}} x_2$$

  Small values of $|\frac{\partial f_1}{\partial x_2}|$ indicate the practical impossibility to apply the inversion operator, which prevents the observation of $x_2(t)$ and, because of the logical sequence, of $x_3(t)$.

- $\frac{\partial f_2}{\partial x_3} \neq 0 \ \forall([x_1, x_2, u])$, so that it is possible to apply the operator:

$$f_2 \xrightarrow[{[x_1, x_2, u]}]{\text{inv}} x_3$$

  Small values of $|\frac{\partial f_2}{\partial x_3}|$ indicate the practical impossibility to apply the inversion operator, which prevents the observation of $x_3(t)$.

- x_1, x_2, and x_3 are such that:

$$|x_1| < X_1$$
$$|x_2| < X_2$$
$$|x_3| < X_3$$

  where X_1, X_2 and X_3 are design constants. These conditions are related with the peaking phenomenon generated because the second differentiator operator in the logical sequence operates with an estimated value $\hat{x}_2(t)$. Condition $|x_3| < X_3$ is introduced to account for a third order differentiator that – as will be shown with the CSTR example in the numerical simulations of Section VI – can be used to estimate a model parameter.

The logical sequence of operators to solve the problem is:

$$g_1 \xrightarrow[{[x_1, u_1]}]{\text{dif}} \hat{f}_1 \xrightarrow[{[x_1, u]}]{\text{inv}} \hat{x}_2 \xrightarrow[{[x_1, \hat{x}_2, u]}]{\text{dif}} \hat{f}_2 \xrightarrow[{[x_1, \hat{x}_2, u]}]{\text{inv}} \hat{x}_3$$

where the notation $\hat{x}$ denotes the estimation of x.

Note that this graphical representation also facilitates the introduction of new nodes, where one node could represent not only states, but estimations and functions, and new operators that can be used to solve the problem. The relation from one node to other node (i.e. the arc) would depend on the type of operator and its associated restrictions. For example, adding a filtering operator to the graphical representation would allow filtering the noisy signal from the origin node, which represents the raw state signal, to the destiny node, which represents the filtered signal.

III. DIFFERENTIATOR DESIGN: THE SMOOTH NONLINEAR SUPER-TWISTING APPROXIMATION

Consider a first-order dynamical system of the form:

$$\dot{x}(t) = f(x) + d(t) \tag{2}$$

where $f(x)$ is known and $d(t)$ is unknown with the following assumption:

Assumption 1: $d(t)$ in (2) satisfies the following restriction

$$|\dot{d}(t)| \leq \Delta$$

with $\Delta > 0$ a positive real number.

Our goal is to obtain the estimation of the variable derivative. A comparative study of techniques to solve this problem can be found in [54], where the following issues are considered:

- Measurement noise and sampling period can affect the exactness of any differentiator.

- There is always a trade-off between the exactness and the robustness of a differentiator.
- In many applications, it is necessary to utilize some noise filtering elements before a differentiator block.

Due to the trade-off between noise filtering and phase lag of a linear filter, it is necessary to decrease its cut-off frequency in order to improve its noise filtering performance. In cascade connections of linear differentiators this phase-lag is transmitted to higher order elements. Solutions like sliding mode or homogeneous differentiators have been introduced in the literature to overcome the drawbacks of the aforementioned methods, but implicit discretization procedures are needed to keep the nonlinear properties of the discrete model. In this work we propose a different approach, based on smooth nonlinear function approximations that maintain the continuous properties in the discrete model.

To this end, note that classical linear algorithms are less sensitive to measurement noise but less robust to perturbation [55], so nonlinear terms can be introduced to improve the performance with respect to perturbations. To this end, let us define the state estimation error as:

$$e(t) = x(t) - \hat{x}(t) \tag{3}$$

We propose a differentiator (observer of the variable derivative) with the following dynamics:

$$\dot{\hat{x}}(t) = f(x) + \lambda e(t) + \beta \tanh(\gamma e(t)) + \epsilon(t)$$
$$\dot{\epsilon}(t) = \frac{\lambda^2}{4} e(t) + \frac{\lambda}{2} \beta \gamma \operatorname{sech}^2(\gamma e(t)) e(t) \tag{4}$$

and initial conditions:

$$\hat{x}(0) = x(0) \quad \epsilon(0) = 0 \tag{5}$$

Note that the observer dynamics (4) shares the structure with the *Super-Twisting Algorithm*, see [44], [56], [57], designed as a differentiator, which are given as:

$$\dot{\hat{x}}(t) = f(x) + \lambda \sqrt{|e(t)|} \operatorname{sign}(e(t)) + \epsilon(t)$$
$$\dot{\epsilon}(t) = \kappa \operatorname{sign}(e(t)) \tag{6}$$

The set value ($\operatorname{sign}(e(t))$) and the power factor ($|e(t)|^{0.5}$) used in (6) are replaced in (4) with a combination of linear and nonlinear functions. Hence we refer to this algorithm as *Smooth Nonlinear Super-Twisting Approximation (SNSTA)*.

From (3) and (4), the dynamics of $e(t)$ are given as:

$$\dot{e}(t) = -\lambda e(t) - \beta \tanh(\gamma e(t)) - \epsilon(t) + d(t)$$
$$\dot{\epsilon}(t) = \frac{\lambda^2}{4} e(t) + \frac{\lambda}{2} \beta \gamma \operatorname{sech}^2(\gamma e(t)) e(t) \tag{7}$$

An important difference of the proposed SNSTA with respect to the ST differentiator is that the final estimate of the variable derivative is obtained from the approximate equilibrium condition (13), ($\dot{e}(t), e(t)) \approx (0, 0)$; that is, assuming the condition:

$$\epsilon(t) \approx d(t). \tag{8}$$

Therefore, the estimation of $\dot{x}(t)$ is obtained in the same way as in the case of a nonlinear observer estimation approach, that is:

$$\dot{x}(t) \approx f(x) + \epsilon(t) \tag{9}$$

This choice reduces the amount of chattering and the sensitivity of the algorithm to high frequency noise in the measured input.

Consider (7), assumption (1) and the linear manifold $\sigma(t)$ defined as:

$$\sigma(t) = \dot{e}(t) + \frac{\lambda}{2} e(t) \tag{10}$$

Theorem 1: The compact set Ω_σ defined as:

$$\Omega_\sigma = \{\sigma(t) \in \mathbb{R} : |\sigma(t)| < \nu_\sigma\} \tag{11}$$

with ν_σ given as:

$$\nu_\sigma = \frac{\Delta}{\frac{\lambda}{2} + \beta \gamma \operatorname{sech}^2(\gamma e(t))} \tag{12}$$

is Globally Uniformly Asymptotically Stable (GUAS).

Proof: Differentiation of $e(t)$ leads to:

$$\dot{e}(t) = f(x) + d(t) - \dot{\hat{x}}(t)$$

Replacing $f(t)$ from (4), we obtain:

$$\dot{e}(t) = -\lambda e(t) - \beta \tanh(\gamma e(t)) - \epsilon(t) + d(t) \tag{13}$$

Let us now differentiate $\dot{e}(t)$ again:

$$\ddot{e}(t) = -\lambda \dot{e}(t) - \frac{\lambda^2}{4} e(t) - \beta \gamma \operatorname{sech}^2(\gamma e(t)) \dot{e}(t)$$
$$- \frac{\lambda}{2} \beta \gamma \operatorname{sech}^2(\gamma e(t)) e(t) + \dot{d}(t) \tag{14}$$

We choose $V(\sigma) = \frac{1}{2} \sigma^2$ as a candidate Lyapunov function. Its derivative is:

$$\dot{V}(\sigma) = \sigma(\ddot{e}(t) + \frac{\lambda}{2} \dot{e}(t)) \tag{15}$$

Replacing $\ddot{e}(t)$ from (14) yields:

$$\dot{V}(\sigma) = -\sigma((\frac{\lambda}{2} + \beta \gamma \operatorname{sech}^2(\gamma e(t)) \sigma(t) - \dot{d}(t)) \tag{16}$$

Condition (12) and assumption (1) implies that:

$$|\frac{\lambda}{2} + \beta \gamma \operatorname{sech}^2(\gamma e(t))||\sigma(t)| > |\dot{d}(t)|, \quad \forall \sigma(t) \notin \Omega_\sigma \tag{17}$$

so that:

$$(\frac{\lambda}{2} + \beta \gamma \operatorname{sech}^2(\gamma e(t))) \sigma(t) - \dot{d}(t) = \rho(t) \sigma(t) \tag{18}$$

with $\rho(t) > 0$. Thus, $\dot{V}(\sigma)$ can be written as:

$$\dot{V}(\sigma) \leq -\rho(t) V(\sigma) \quad \forall \sigma \notin \Omega_\sigma \tag{19}$$

which implies that Ω_σ generates exponential convergence (with time variable rate $\rho(t)$) with respect to $\sigma(t)$.

Theorem 2: Let us define

$$\psi < \operatorname{atan}(\frac{\lambda}{2}) \tag{20}$$

The compact set Ω_e defined as:

$$\Omega_e = \{(e(t), \dot{e}(t)) \in \mathbb{R}^2 : |e(t)| < \frac{v_\sigma}{|\sin(\psi)|} \wedge |\dot{e}(t)|$$
$$< \frac{v_\sigma}{|\cos(\psi)|}\} \qquad (21)$$

is Global Uniform Asymptotically Stable (GUAS).

Proof: Inside Ω_σ the following condition holds:

$$|\dot{e}(t) + \frac{\lambda}{2}e(t)| < v_\sigma$$

which geometrically entails:

$$|e(t)| < \frac{v_\sigma}{|\sin(\psi)|} \qquad (22)$$

$$|\dot{e}(t)| < \frac{v_\sigma}{|\cos(\psi)|} \qquad (23)$$

Theorem 3: The compact set Ω_σ^* defined as:

$$\Omega_\sigma^* = \{\sigma(t) \in \mathbb{R} : |\sigma(t)| < v_\sigma^*\} \qquad (24)$$

with v_σ^* given as:

$$v_\sigma^* = \frac{\Delta}{\beta\gamma \, \text{sech}^2(\gamma e(t))} \qquad (25)$$

is Finite Time Stable (FTS).

Before introducing the proof, let us recall the following result introduced in [58]:

Lemma 1: For any real numbers $\psi_1 > 0$, $\psi_2 > 0$ and $0 < \psi_3 < 1$, an extended Lyapunov function condition of finite time stability can be given as

$$\dot{V}(x) + \psi_1 V(x) + \psi_2 V^{\psi_3}(x) \le 0 \qquad (26)$$

where the settling time can be estimated by

$$T \le \frac{1}{\psi_1(1-\psi_3)} \ln\left(\frac{\psi_1 V^{(1-\psi_3)}(0) + \psi_2}{\psi_2}\right) \qquad (27)$$

Proof: By definition (25),

$$|\beta\gamma \, \text{sech}^2(\gamma e(t))||\sigma(t)| > |\dot{d}(t)|, \quad \forall \sigma \notin \Omega_\sigma^*$$

Therefore,

$$-\beta\gamma \, \text{sech}^2(\gamma e(t))\sigma(t) + \dot{d}(t) = -\phi(t) \, \text{sign}(\sigma(t)),$$
$$\forall \sigma \notin \Omega_\sigma^*$$

with $\phi(t) > 0$. In this case the derivative of the Lyapunov function (16) follows the expression:

$$\dot{V}(\sigma) \le -\frac{\lambda}{2}V(x) - \phi(t)V^{0.5}(\sigma), \quad \forall \sigma \notin \Omega_\sigma^* \qquad (28)$$

Therefore, Lemma (1) implies that Ω_σ^* generates a finite time convergence with variable rate.

The following remarks are in order:

- $\Omega_\sigma \subset \Omega_\sigma^* \, \forall e(t)$. Exponential convergence changes from finite time to asymptotic time inside $\Omega_\sigma \cap \Omega_\sigma^*$.
- $|e(t)| \rightarrow 0$ implies that:

$$v_\sigma \rightarrow \frac{\Delta}{\frac{\lambda}{2} + \beta\gamma} \qquad (29)$$

$$v_\sigma^* \rightarrow \frac{\Delta}{\beta\gamma} \qquad (30)$$

- $|e(0)| \approx 0$ when the initial value of the estimation variable can be estimated with a given minimum accuracy. Therefore, the peaking phenomenon will not affect the proposed differentiator if the value of $x(t)$ is previously known, as it happens with reduced order observers. Nevertheless, when it is necessary to use a previously estimated value in the differentiation chain, the problem can be overcome by enforcing bounds on the estimated value [27].

IV. DIFFERENTIATOR DESIGN: DISCRETIZATION AND PARAMETER SETTINGS

As discussed in [54], [56], [59]–[62], the discretization of continuous-time systems that include set value or homogeneous functions must be done carefully because:

- The chattering phenomenon is closely related to the discretization method.
- The properties related to set value and homogeneous functions in the continuous analysis should be preserved in the discrete model.

To address these points, it is common to replace the explicit discretization method with an implicit approach, which provides higher stability in the integration process and rejects chattering. Our approach is to use a semi-implicit discretization method in order to introduce parameter restrictions that cancel chattering.

A. DIFFERENTIATOR DISCRETIZATION

The Backward Euler discretization method with fixed sampling time τ yields:

$$e_{k+1} = e_k - \tau(\lambda e_k + \beta \tanh(\gamma e_k) + \epsilon_k - d_k) \qquad (31)$$

$$\epsilon_{k+1} = \epsilon_k + \tau(\frac{\lambda^2}{4}e_k + \frac{\lambda}{2}\beta\gamma \, \text{sech}^2(\gamma e_k)e_k) \qquad (32)$$

A semi-implicit approximation can be obtained by replacing ϵ_k with ϵ_{k+1} in the expression of e_{k+1}, which leads to:

$$e_{k+1} = e_k - \tau(\lambda e_k - \beta \tanh(\gamma e_k) - \epsilon_{k+1} + d_k) \qquad (33)$$

so that:

$$e_{k+1} = e_k - \Delta_k - \tau(\epsilon_k - d_k) \qquad (34)$$

with

$$\Delta_k = \tau((\lambda e_k + \beta \tanh(\gamma e_k))$$
$$+ \tau^2(\frac{\lambda^2}{4}e_k + \frac{\lambda}{2}\beta\gamma \, \text{sech}^2(\gamma e_k)e_k) \qquad (35)$$

B. NOISE-FREE MODEL: PARAMETER SETTINGS

Here we consider a noise-free scenario, in which the differentiator is designed to converge as fast as possible, taking only into account the chattering resulting from the discretization process. This choice presents a trade-off: on the one hand, it is desirable to set these gains to high values, in order to obtain a fast observer. On the other hand, they cannot be

too large, in order to avoid chattering at the steady-state of the estimation error. Hence, in this section we calculate the bounds for the gains λ, β, and γ that prevent chattering for a fixed sampling time τ.

It can be shown that:

$$|\Delta_k| \leq (\tau(\lambda + \beta\gamma) + \tau^2(\frac{\lambda^2}{4} + \frac{\lambda}{2}\beta\gamma))|e_k| \qquad (36)$$

Assuming that $\tau(\epsilon_k - d_k)$ is negligible in (34) when $|e_k|$ is small, we introduce two restrictions to cancel the chattering caused by finite time discretization:

$$(\lambda + \beta\gamma) < \frac{1}{2\tau} \qquad (37)$$

$$(\frac{\lambda^2}{4} + \frac{\lambda}{2}\beta\gamma) < \frac{1}{2\tau^2} \qquad (38)$$

which implies that $|\Delta_k| < 1$. Thus, $\text{sign}(e_{k+1}) = \text{sign}(e_k)$ when $|e_k|$ is small and $\tau(\epsilon_k - d_k)$ is negligible. Choosing

$$\beta\gamma = \lambda, \qquad (39)$$

the restriction

$$\lambda < \frac{1}{4\tau} \qquad (40)$$

yields the desired condition, $|\Delta_k| < 1$.

The parameter γ should be selected as large as possible, to achieve a good approximation of the sign function but without causing chattering. Its value is obtained as:

$$\gamma = \frac{1}{2\tau} \qquad (41)$$

In case of noisy models, the values of the parameters should be modified with respect to a required cut-off frequency designed to filter high frequency noisy signals, thus introducing a frequency domain approach to determine the values of the parameters.

C. CUT-OFF FREQUENCY DESIGN
Note that if the nonlinear terms in (14) are canceled, the transfer function from $d(t)$ to $e(t)$ is given as:

$$G_{de}(s) = \frac{Z(s)}{D(s)} = \frac{s}{(s + \frac{\lambda}{2})^2} \qquad (42)$$

which resembles the full-order observer transfer function obtained in [27] (*page 11*) for a second order system. This means that, if $d(t)$ is corrupted by noise, the proposed observer will have a good attenuation of high-frequency *disturbance* signals. Transfer function $G_{de}(s)$ implies that:

$$\lambda = 2\omega_c \qquad (43)$$

where ω_c is chosen as the desired cut-off frequency. Applying (40), a bound for the application of the algorithm is:

$$\omega_c \leq \frac{1}{8\tau} \qquad (44)$$

D. PEAKING PHENOMENON REDUCTION
The frequency design approach allow us to introduce a modification that reduces the peaking phenomenon, which, as in the case of chattering, is related to high frequency oscillations. To reduce the impact of peaking, adaptive values of the cut-off frequency are used in the high order elements of the differentiators chain. In this way, besides the introduction of saturation in the states estimations, a reduced value of the cut-off frequency when the differentiator is affected by peaking is used as a high frequency filter that attenuates the oscillations. Thus, in the simulations the cut-off frequencies of the second and third differentiators are chosen as:

$$\omega_{c_2} = \omega_{c_1}((1 - \alpha) + \alpha(1 - e^{-\kappa_2 t})) \qquad (45)$$

$$\omega_{c_3} = \omega_{c_1}((1 - \alpha) + \alpha(1 - e^{-\kappa_3 t})) \qquad (46)$$

with $\alpha = 0.80$, $\kappa_2 = 0.25$, $\kappa_3 = 0.1$, and ω_{c_1} the chosen cut-off frequency for the first differentiator.

In the noise free case, ω_{c_1} is chosen to be equal to the limit cut-off frequency:

$$\omega_{c_1} = \frac{1}{8\tau} \frac{rad}{s} \qquad (47)$$

such that it is used to test the chattering cancellation caused by discretization.

V. OBSERVABILITY
The theoretical possibility of inferring the internal state of a system by observing its output is defined by the property of observability. Thus, it is advisable to assess this property before designing an observer. The observability of nonlinear systems can be analyzed with differential geometry methods. In particular, it can be checked by calculating the rank of the (generalized) observability matrix. Let us write our nonlinear models in the following general form:

$$M_{NL} := \begin{cases} \dot{x}(t) = f(x(t), \theta, u(t), w(t)), \\ y(t) = h(x(t), \theta, u(t), w(t)), \\ x(t_0) = x^0(\theta) \end{cases} \qquad (48)$$

where $\theta \in \mathbb{R}^q$ is the unknown parameter vector, $u(t) \in \mathbb{R}^{m_u}$ is the known input, $w(t) \in \mathbb{R}^{m_w}$ the unknown external disturbances, $x(t) \in \mathbb{R}^m$ the state vector, $y(t) \in \mathbb{R}^n$ the output vector, and f and h analytical functions.

Unknown parameters and inputs can be considered as unmeasured states. While parameters are constant, unknown inputs can be time-varying. Thus, they can be included in an augmented state vector as follows:

$$\tilde{x}(t) = \begin{bmatrix} x(t) \\ \theta \\ w(t) \end{bmatrix}, \quad \dot{\tilde{x}}(t) = \begin{bmatrix} f(\tilde{x}(t), u(t)) \\ 0 \\ \dot{w}(t) \end{bmatrix}. \qquad (49)$$

The observability matrix of the system defined above can be built with Lie derivatives of the output function. The Lie derivative of $h(\tilde{x})$ with respect to $f(\tilde{x})$ is given by:

$$L_f h(\tilde{x}) = \frac{\partial h(\tilde{x})}{\partial \tilde{x}} f(\tilde{x}, u) + \sum_{j=0}^{\infty} \frac{\partial h(\tilde{x})}{\partial u^{(j)}} u^{(j+1)}, \qquad (50)$$

where $u^{(j)}$ stands for the jth derivative of u. The Lie derivatives of higher orders can be obtained recursively as follows:

$$L_f^i h(\widetilde{x}) = \frac{\partial L_f^{i-1} h(\widetilde{x})}{\partial \widetilde{x}} f(\widetilde{x}, u) + \sum_{j=0}^{\infty} \frac{\partial L_f^{i-1} h(\widetilde{x})}{\partial u^{(j)}} u^{(j+1)}. \quad (51)$$

We can now define the observability matrix of the system as follows:

$$\mathcal{O}(\widetilde{x}, u) = \begin{pmatrix} \frac{\partial}{\partial \widetilde{x}} h(\widetilde{x}, u) \\ \\ \frac{\partial}{\partial \widetilde{x}}(L_f h(\widetilde{x}, u)) \\ \\ \frac{\partial}{\partial \widetilde{x}}(L_f^2 h(\widetilde{x}, u)) \\ \vdots \\ \frac{\partial}{\partial \widetilde{x}}(L_f^{n_{\widetilde{x}}-1} h(\widetilde{x}, u)) \end{pmatrix}. \quad (52)$$

And the observability of model (48) is given by the observability condition: if the above matrix has full rank, i.e. $rank(\mathcal{O}(\widetilde{x}_0, u)) = m+q+m_w$, where $\widetilde{x}_0$ is a (possibly generic) point in the augmented state space, then the model is fully observable in a neighbourhood $\mathcal{N}(\widetilde{x}_0)$ of $\widetilde{x}_0$. [63].

VI. CASE STUDIES: NUMERICAL SIMULATIONS
In this section we apply our methodology to two models of dynamical systems. First, we analyze their observability with the MATLAB toolbox STRIKE-GOLDD [63], which automatically builds matrix (52) and checks the observability condition. In both cases we obtain that the models are observable. Next, we design an observer using the proposed approach.

We compare the results of our smooth nonlinear super-twisting approximation algorithm (**SNSTA**) with those obtained with the super-twisting differentiator (**ST**), and with the cascade high-gain observer (**KC**) proposed in [49]. In this case, a coordinate transformation to generate a normal form compatible with [49] needs to be introduced. Consider the following transformation:

$$v_1 = x_1$$
$$v_2 = \dot{x}_1$$
$$v_3 = \ddot{x}_1$$

The structure of the cascade high-gain observer to estimate $v = [v_1, v_2, v_3]^T$ is given as:

$$\dot{z}_1 = (\frac{1}{\epsilon})[z_2 + 2(y - z_1)]$$
$$\dot{z}_2 = (\frac{1}{\epsilon})(y - z_1)$$
$$\dot{z}_3 = -(\frac{1}{\epsilon})(z_3 + \hat{v}_2)$$

where

$$\hat{v}_1 = z_1$$

$$\hat{v}_2 = M_2 sat(\frac{z_2}{\epsilon M_2})$$
$$\hat{v}_3 = M_3 sat(\frac{z_3 + \hat{v}_2}{\epsilon M_3})$$

In order to transform $\hat{v}$ into the original coordinates x, note that v can be written as:

$$v_1 = x_1$$
$$v_2 = f_1 + g_1$$
$$v_3 = \dot{f}_1 + \dot{g}_1$$

Therefore, the estimation of x_2 it is obtained as

$$\hat{x}_2 = f_1^{-1}(\hat{v}_2 - g_1)$$

where f_1^{-1} denotes the inverse of the function f_1 with respect to x_2. The estimation of x_3 depends on the expressions of $\dot{f}_1$ and $\dot{g}_1$ that must be obtained for each case study.

In the next subsections, we show numerical simulations using a fixed sampling time $\tau = 0.01$.

Besides the noise free model scenario, we introduce two cases where the measurements are corrupted by different types of noise, given as follows:

- **White Gaussian noise.** Following [54], we add white noise to the input signal using the MATLAB command `y = awgn(x,SNR,'measured')`, where x is the input signal, y is the polluted signal, and SNR is the signal-to-noise ratio. In this case, the differentiator is configured by selecting a cut-off frequency that provides a good trade-off between filtering and tracking properties, that is, low sensitivity to noise and good reproduction of the underlying signal with minimal time lag. In the simulations we set SNR = 30 dB, as in [54].
- **High frequency harmonic noise.**
  In this case, as in [5], a high-frequency harmonic signal with a large amplitude is considered as noise:

$$n(t) = N(\cos(\omega_n t) + 0.83 \sin(1.29\omega_n t - 0.14)$$
$$+0.23 \cos(5.12\omega_n t + 0.26)$$
$$+0.65 \cos(3.37\omega_n t + 0.36)e^{\cos(1.21\omega_n t + 0.13)}) \quad (53)$$

where $N = 0.25$ is the noise amplitude and $\omega_n = 80\frac{rad}{s}$ is the noise base frequency.

In the case of noisy measures, ω_{c_1} is set to:

$$\omega_{c_1} = 8\frac{rad}{s} \quad (54)$$

A. FITZHUGH-NAGUMO
Our first case study is the modified Fitzhugh-Nagumo model presented in [22] (*page 107*), the dynamics of which is given by:

$$\dot{V}(t) = V(t) - \frac{V^3(t)}{3} - W(t)$$
$$\dot{W}(t) = \epsilon(g(V) - W(t) - \eta)$$

where

$$g(V) = \begin{cases} \alpha_V V(t) & \text{if } V(t) > 0 \\ \beta_V V(t) & \text{if } V(t) \le 0 \end{cases}$$

The model contains two states, one of which $(V(t))$ is the measured output, and four parameters, two of which (α_V and β_V) are unknown. Since α_V and β_V play the same role in the dynamics, for the purpose of observability analysis they can be seen as the same parameter with different values in separate regions. Therefore, for the model to be fully observable, the rank of matrix (52) should be three (two states plus one parameter). The analysis with STRIKE-GOLDD yields that this is indeed the case, so we proceed to the observer design. The objective is to develop an estimator of $W(t)$ and $g(V)$ using the information of the measured output, $V(t)$, and the knowledge of parameters ϵ and η.

In order to define the restrictions of the logical sequence of operators, the state space is assumed to be constrained by:

$$|V(t)| < 4.0 \quad |W(t)| < 5.0$$

In the graphical results of the numerical simulations it will be shown that these are conservative assumptions, i.e. the chosen values overestimate the real limits. These bounded state space assumptions lead to the following inequality:

$$|g(V)| \le \beta_V|V(t)| < 7.84$$

The modified Fitzhugh-Nagumo model can be written in the form (1) by choosing:

$$x_1(t) = V(t)$$
$$x_2(t) = W(t)$$
$$x_3(t) = g(V)$$

and

$$f_1 = -x_2$$
$$g_1 = x_1 - \frac{x_1^3}{3}$$
$$f_2 = \epsilon x_3$$
$$g_2 = -\epsilon(x_2 + \eta)$$

The model dynamics is such that:

$$\dot{f}_1 = -f_2 - g_2$$
$$\dot{g}_1 = (f_1 + g_1)(1 - y^2)$$

The estimation of x_3 provided by cascade high-gain observer is obtained as:

$$\hat{x}_3 = f_2^{-1}(-\hat{v}_3 - \hat{g}_2 + \hat{v}_2(1 - y^2))$$

where f_2^{-1} denotes the inverse of the function f_2 with respect to x_3.

In the numerical simulations we use the parameter values shown in Table 1, and the initial conditions $x_1(0) = 1.0656$, $x_2(0) = 2.6903$ and $x_3(0) = 2.0886$.

First we assess the performance of the compared differentiators in the noise free case. Results are shown in

TABLE 1. Parameters of the Fitzhugh-Nagumo model.

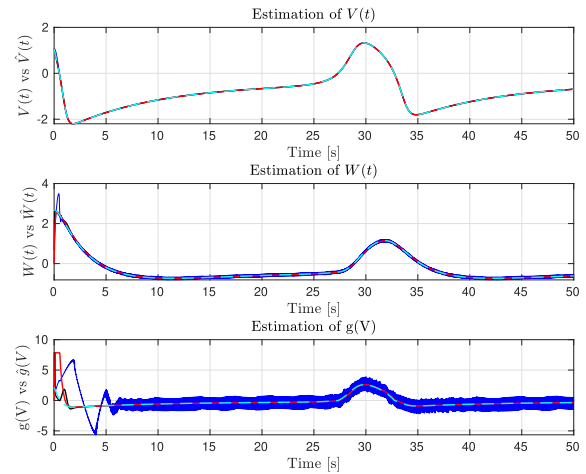| Parameter	Value
η	0.20531
ϵ	0.2966
α_V	0.50
β_V	1.96

FIGURE 2. Fitzhugh-Nagumo model without noise: trajectories of the states $V(t)$, $W(t)$ and $g(V(t))$, along with their estimations ($\hat{*}$). **Dashed cyan lines**: true trajectories of $V(t)$, $W(t)$ and $g(V(t))$; **red lines**: estimates obtained with the observer proposed in the present work; black lines: estimates obtained with the observer proposed in [49]; **blue lines**: estimates obtained with the super-twisting algorithm.

Figures 2–3. Figure 2 displays the time course of the states and their estimations $\hat{W}(t)$ and $\hat{g}(V)$, and Figure 3 shows a detailed view of the initial responses.

While algorithms KC and SNSTA are able to estimate $V(t)$, $W(t)$ and $g(V)$ without significant chattering or time lag, ST generates some appreciable chattering in $\hat{g}(V)$.

Figure 4 shows the results obtained when white Gaussian noise corrupts the measured state and the desired cut-off frequency. Algorithms KC and SNSTA are able to estimate $V(t)$ and $W(t)$ with high robustness and very good performance between noise sensitivity and introduced time lag, but ST generates some chattering in $\hat{W}(t)$. Estimation of $g(V)$ shows a small amount of time lag and a certain level of high frequency signals, but SNSTA provides less time lag than KC and better chattering attenuation than ST.

Figure 5 shows the results obtained when the high frequency harmonic noise corrupts the measured state, with the same cut-off frequency. In this case the ST algorithm is not used, due to the large amount of chattering that it introduces.

B. CONTINUOUS STIRRED-TANK REACTOR (CSTR)
In this example we apply the proposed method to the CSTR model described in [64], which we modify by assuming that $T_r(t)$ is not measurable. The model equations are:

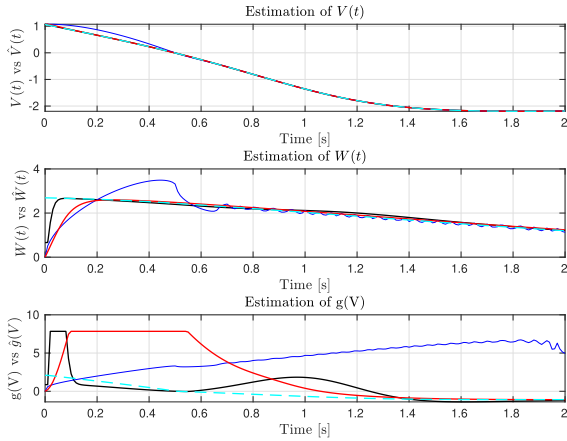$$\dot{C}_r(t) = Q(U_1 - C_r(t)) - 0.072F(T_r)C_r(t) + d(t)$$

FIGURE 3. Fitzhugh-Nagumo model without noise: time courses of the states for $t \in [0, 2]$. **Dashed cyan lines**: true trajectories of $V(t)$, $W(t)$ and $g(V(t))$; **red lines**: estimates obtained with the observer proposed in the present work; **black lines**: estimates obtained with the observer proposed in [49]; **blue lines**: estimates obtained with the super-twisting algorithm.
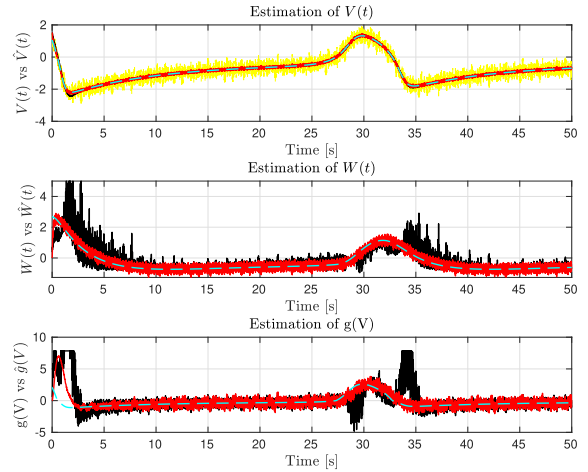

FIGURE 4. Fitzhugh-Nagumo model with Gaussian noise: trajectories of the states $V(t)$, $W(t)$ and $g(V(t))$, along with their estimations (✱). **Dashed cyan lines**: true trajectories of $V(t)$, $W(t)$ and $g(V(t))$; **red lines**: estimates obtained with the observer proposed in the present work; **black li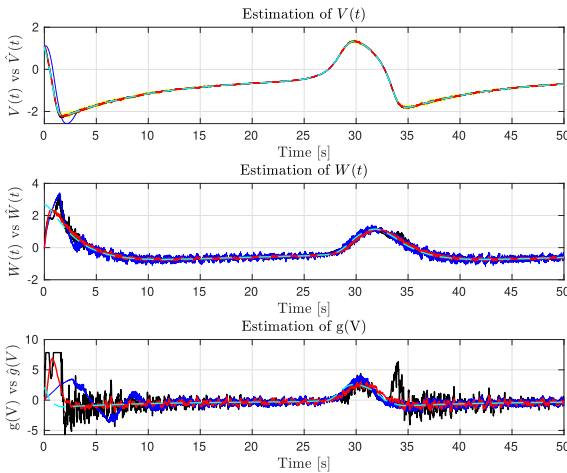nes**: estimates obtained with the observer proposed in [49]; **blue lines**: estimates obtained with the super-twisting algorithm.

$$\dot{T}_r(t) = Q(U_2 - T_r(t)) + 0.576 F(T_r) C_r(t)$$
$$\quad\quad -0.3(T_r(t) - T_c(t))$$
$$\dot{T}_c(t) = \delta_1 Q_C(U_3 - T_c(t)) + 3.0(T_r(t) - T_c(t))$$
$$y(t) = T_c(t)$$

with

$$F(T_r) = \exp^{\left(\frac{\gamma T_r}{\gamma + T_r}\right)}$$

In this model, the variable $C_r(t)$ is the concentration of the chemical reactive, $T_r(t)$ is the reactor temperature, and $T_c(t)$ is the cooled jacket temperature. The observed variable is $T_c(t)$, and there is an external disturbance $d(t)$. The model parameters are assumed known. Thus, for the purpose of observability analysis the model has one output, three states

FIGURE 5. Fitzhugh-Nagumo model with high frequency harmonic noise: trajectories of the states $W(t)$ and $g(V(t))$, along with their estimations (✱). **Dashed cyan lines**: true trajectories of $V(t)$, $W(t)$ and $g(V(t))$; **red lines**: estimates obtained with the observer proposed in the present work; **black lines**: estimates obtained with the observer proposed in [49].

TABLE 2. Parameters of the CSTR model.

Parameter	Value
Q	1
Q_C	0.28
δ_1	10
γ	2.0
U_1	1
U_2	0
U_3	-1

and one unknown input. If we assume that $d(t)$ is a polynomial function with a finite number of nonzero derivatives, the analysis concludes that the model is fully observable.

In the design of the observer the first objective is to estimate $T_r(t)$, $C_r(t)$ from the dynamics of $\dot{T}_r(t)$ and $\dot{T}_c(t)$. Then, the external disturbance $d(t)$ is estimated from the dynamics of $\dot{C}_r(t)$ applying a differentiator operator. The model can be written in form (1) choosing:

$$x_1(t) = T_c(t)$$
$$x_2(t) = T_r(t)$$
$$x_3(t) = C_r(t)$$

and

$$f_1 = 3.0\, x_2$$
$$g_1 = \delta_1 Q_C(U_3 - x_1) - 3.0\, x_1$$
$$f_2 = 0.576 F(x_2) x_3$$
$$g_2 = Q(U_2 - x_2) - 0.3(x_2 - x_1)$$

We assume that the states are bounded as follows:

$$|T_c(t)| < 5.0 \quad |T_r(t)| < 4.0\ |C_r(t)| < 4.0$$

The initial conditions are $x_1(0) = 0.12$, $x_2(0) = 2.67$, and $x_3(0) = 0.58$. The parameter values used for simulations are shown in Table 2.
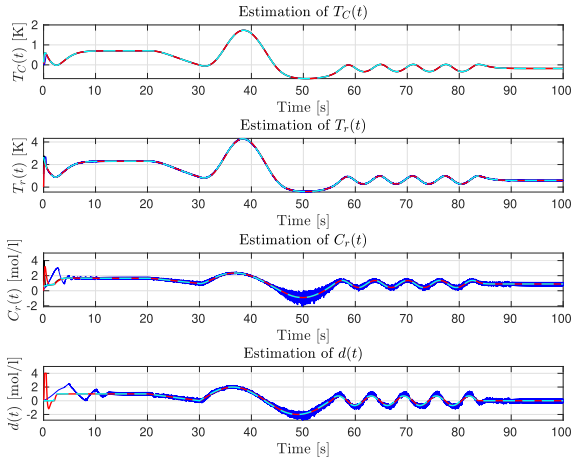
FIGURE 6. CSTR model without noise: numerical simulations of the state estimation. Full trajectory of $T_c(t)$, $T_r(t)$ and $C_r(t)$, and of the unknown disturbance $d(t)$, as well as of their estimations (⋇). **Dashed cyan lines:** $T_c(t)$, $T_r(t)$, $C_r(t)$ and $d(t)$; **red lines:** estimates obtained with the observer proposed in the present work; black lines: estimates obtained with the observer proposed in [49]; **blue lines:** estimates obtained with the super-twisting algorithm.
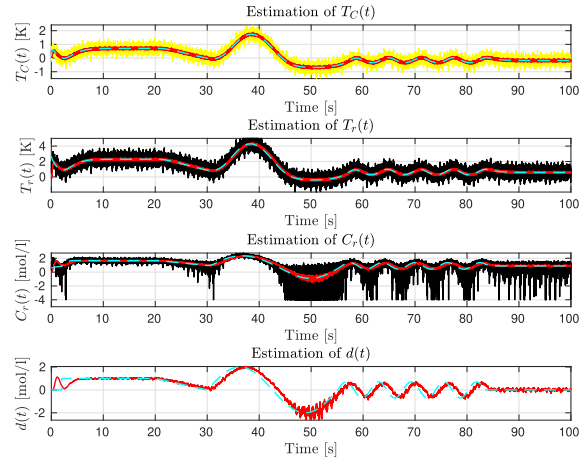

FIGURE 8. CSTR model without with high frequency harmonic noise: numerical simulations of the state estimation. Full trajectory of $T_c(t)$, $T_r(t)$ and $C_r(t)$, and of the unknown disturbance $d(t)$, as well as of their estimations (⋇). **Dashed cyan lines:** $T_c(t)$, $T_r(t)$, $C_r(t)$ and $d(t)$; **red lines:** estimates obtained with the observer proposed in the present work; black lines: estimates obtained with the observer proposed in [49];.
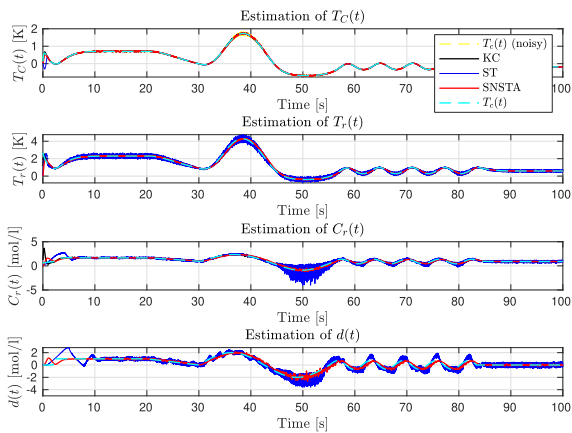

FIGURE 7. CSTR model with Gaussian noise: numerical simulations of the state estimation. Full trajectory of $T_c(t)$, $T_r(t)$ and $C_r(t)$, and of the unknown disturbance $d(t)$, as well as of their estimations (⋇). **Dashed cyan lines:** $T_c(t)$, $T_r(t)$, $C_r(t)$ and $d(t)$; **red lines:** estimates obtained with the observer proposed in the present work; black lines: estimates obtained with the observer proposed in [49]; **blue lines:** estimates obtained with the super-twisting algorithm.

We apply the cascade high-gain observer to the model dynamics,

$$\dot{f}_1 = 3(f_2 + g_2)$$
$$\dot{g}_1 = -(\delta_1 Q_C + 3)(f_1 + g_1),$$

obtaining the estimation of x_3 as:

$$\hat{x}_3 = f_2^{-1}((\frac{1}{3})(\hat{v}_3 - 3\hat{g}_2 + (\delta_1 Q_C + 3)\hat{v}_2))$$

where f_2^{-1} denotes the inverse of the function f_2 with respect to x_3.

The results obtained in the noise free case are shown in Figure 6. We have used the differentiator operator to estimate

the value of the external disturbance $d(t)$ from the dynamics of $\dot{C}_r(t)$, which is known. The conclusions are similar to the first example for $\hat{T}_r(t)$ and $\hat{C}_r(t)$. In the case of $\hat{d}(t)$, it can be noticed that, as the depth in the logical sequence of estimation increases, the peaking phenomenon is more pronounced and the estimation is more sensitive to errors in the previous stage of the logical sequence.

Figures 7 and 8 show the results obtained in the noisy scenarios (resp., with Gaussian and high frequency harmonic noises). It can be observed that the SNSTA solution provides better performance, reducing chattering and time lag, at least up to the third estimation.

VII. DISCUSSION AND CONCLUSION

In this work we have proposed an approach to develop nonlinear observers for a class of nonlinear dynamical systems. The methodology consists on the successive application of two operators, differentiation and inversion. The logical sequence of operations is derived from a graph of the relationships among the variables and functions of the dynamical system. Traversing this graph, we obtain a path from the known quantities to the unknowns that need to be estimated. Progress along the path entails applying, at each step, either the differentiator or the inversion operator. The application of the inversion operator requires that certain conditions are fulfilled. More specifically, in order to solve the observation problem the dynamics must have non-zero sensitivity to changes in the unmeasured states.

The main goal of the methodology is to avoid two undesirable phenomena, peaking and chattering. The first one is prevented by introducing bounds on a saturation term included in the differentiator. The second one is avoided by tuning the design parameters λ, β and γ, which are directly related with the desired cur-off frequency and with the sampling time.

We introduce as a restriction an upper bound on the derivative of the unknown term in the dynamic equation (Δ). Note that, if we consider $d(t)$ as an external disturbance (instead of a internal unknown state), the value of Δ in Section III can be estimated from the filtering properties of a second order dynamic system. Any frequency higher than this *cut-off frequency value* present in $d(t)$ will not affect the response obtained.

In future work, we plan to investigate the use of nonlinear high frequency filtering techniques for attenuating the time lag caused by noisy signals, and to scale the technique to handle more complex dynamic networks, as well as to develop an extended graph representation in order to define observability maps based on system state and operator restrictions, which will bring the methodology closer to machine learning optimization techniques.

DATA AND CODE AVAILABILITY
The MATLAB code of the numerical simulations presented in this paper is available at:

https://github.com/jagprieto/high_gain_observers_chemical/. The implementation of the numerical simulations is included in the file `simulations.m`

The observability analysis of the case studies was performed with the MATLAB toolbox STRIKE-GOLDD, which is available at https://github.com/afvillaverde/strike-goldd. The implementations of the case studies are included in the models folder, with the names `FHN_observer.mat` and `CSTR_observer.mat`

DECLARATION OF COMPETING INTEREST
The authors declare that they have no known competing financial interests or personal relationships that could have appeared to influence the work reported in this paper.

CREDIT AUTHORSHIP CONTRIBUTION STATEMENT
José Antonio González-Prieto: Conceptualization, Investigation, Methodology (observer design), Software (numerical simulations), Formal analysis, Writing – original draft, Writing – Review & Editing. **Alejandro F. Villaverde:** Formal analysis, Methodology (observability analysis), Software (observability analysis), Funding acquisition, Writing – original draft, Writing – Review & Editing.

REFERENCES
[1] D. Boutat and G. Zheng, *Observer Design for Nonlinear Dynamical Systems*. Springer, 2021.
[2] A. Levant, "Robust exact differentiation via sliding mode technique," *Automatica*, vol. 34, no. 3, pp. 379–384, Mar. 1998.
[3] B.-Z. Guo and Z.-L. Zhao, "On convergence of tracking differentiator," *Int. J. Control*, vol. 84, no. 4, pp. 693–701, Apr. 2011.
[4] A. Levant, "Filtering differentiators and observers," in *Proc. 15th Int. Workshop Variable Struct. Syst. (VSS)*, Jul. 2018, pp. 174–179.
[5] A. Levant and M. Livne, "Robust exact filtering differentiators," *Eur. J. Control*, vol. 55, pp. 33–44, Sep. 2020.
[6] A. Levant and X. Yu, "Sliding-mode-based differentiation and filtering," *IEEE Trans. Autom. Control*, vol. 63, no. 9, pp. 3061–3067, Sep. 2018.
[7] J. O'Reilly, *Observers for Linear Systems*, vol. 170. New York, NY, USA: Academic, 1983.

[8] F. Yang and R. W. Wilde, "Observers for linear systems with unknown inputs," *IEEE Trans. Autom. Control*, vol. 33, no. 7, pp. 677–681, Jul. 1988.
[9] A. Krener and W. Respondek, "Nonlinear observers with linearizable error dynamics," *SIAM J. Control Optim.*, vol. 23, no. 2, pp. 197–216, 1985.
[10] A. J. Krener and A. Isidori, "Linearization by output injection and nonlinear observers," *Syst. Control Lett.*, vol. 3, no. 1, pp. 47–52, 1983.
[11] H. Shim, Y. I. Son, and J. H. Seo, "Semi-global observer for multi-output nonlinear systems," *Syst. Control Lett.*, vol. 42, no. 3, pp. 233–244, Mar. 2001.
[12] M. Arcak and P. Kokotović, "Nonlinear observers: A circle criterion design and robustness analysis," *Automatica*, vol. 37, no. 12, pp. 1923–1930, 2001.
[13] J.-J. Slotine, J. K. Hedrick, and E. A. Misawa, "On sliding observers for nonlinear systems," *J. Dyn. Syst., Meas., Control*, vol. 109, 1987.
[14] Y. Xiong and M. Saif, "Sliding mode observer for nonlinear uncertain systems," *IEEE Trans. Autom. Control*, vol. 46, no. 12, pp. 2012–2017, Dec. 2001.
[15] J. Barbot, M. Djemai, and T. Boukhobza, "Sliding mode observers," *Sliding Mode Control Eng.*, vol. 11, p. 33, 2002.
[16] H. Hammouri and M. Farza, "Nonlinear observers for locally uniformly observable systems," *ESAIM: Control, Optim. Calculus Variat.*, vol. 9, pp. 353–370, Mar. 2003.
[17] T. Floquet, C. Edwards, and S. K. Spurgeon, "On sliding mode observers for systems with unknown inputs," *Int. J. Adapt. Control Signal Process.*, vol. 21, nos. 8–9, pp. 638–656, 2007.
[18] C. P. Tan, X. Yu, and Z. Man, "Terminal sliding mode observers for a class of nonlinear systems," *Automatica*, vol. 46, pp. 1401–1404, Aug. 2010.
[19] S. Ding, J. H. Park, and C.-C. Chen, "Second-order sliding mode controller design with output constraint," *Automatica*, vol. 112, Feb. 2020, Art. no. 108704.
[20] J. A. González, A. Barreiro, S. Dormido, and A. Baños, "Nonlinear adaptive sliding mode control with fast non-overshooting responses and chattering avoidance," *J. Franklin Inst.*, vol. 354, no. 7, pp. 2788–2815, May 2017.
[21] A. Chakrabarty, A. E. Rundell, S. H. Żak, F. Zhu, and G. T. Buzzard, "Unknown input estimation for nonlinear systems using sliding mode observers and smooth window functions," *SIAM J. Control Optim.*, vol. 56, no. 5, pp. 3619–3641, Jan. 2018.
[22] G. Besançon, *Nonlinear Observers and Applications*, vol. 363. Springer, 2007.
[23] V. Andrieu, L. Praly, and A. Astolfi, "High gain observers with updated gain and homogeneous correction terms," *Automatica*, vol. 45, no. 2, pp. 422–428, Feb. 2009.
[24] J. H. Ahrens and H. K. Khalil, "High-gain observers in the presence of measurement noise: A switched-gain approach," *Automatica*, vol. 45, no. 4, pp. 936–943, Apr. 2009.
[25] K. Kalsi, J. Lian, S. Hui, and S. H. Żak, "Sliding-mode observers for systems with unknown inputs: A high-gain approach," *Automatica*, vol. 46, no. 2, pp. 347–353, Feb. 2010.
[26] N. Boizot, E. Busvelle, and J.-P. Gauthier, "An adaptive high-gain observer for nonlinear systems," *Automatica*, vol. 46, no. 9, pp. 1483–1488, Sep. 2010.
[27] H. K. Khalil and L. Praly, "High-gain observers in nonlinear feedback control," *Int. J. Robust Nonlinear Control*, vol. 24, no. 6, pp. 993–1015, Apr. 2014.
[28] D. Astolfi and L. Marconi, "A high-gain nonlinear observer with limited gain power," *IEEE Trans. Autom. Control*, vol. 60, no. 11, pp. 3059–3064, Nov. 2015.
[29] H. K. Khalil, *High-Gain Observers Nonlinear Feedback Control*. Philadelphia, PA, USA: SIAM, 2017.
[30] H. K. Khalil, "Extended high-gain observers as disturbance estimators," *SICE J. Control Meas. Syst. Integr.*, vol. 10, no. 3, pp. 125–134, 2017.
[31] A. Chakrabarty, M. J. Corless, G. T. Buzzard, S. H. Żak, and A. E. Rundell, "State and unknown input observers for nonlinear systems with bounded exogenous inputs," *IEEE Trans. Autom. Control*, vol. 62, no. 11, pp. 5497–5510, Nov. 2017.
[32] A. Chakrabarty and M. Corless, "Estimating unbounded unknown inputs in nonlinear systems," *Automatica*, vol. 104, pp. 57–66, Jun. 2019.
[33] A. Zemouche, F. Zhang, F. Mazenc, and R. Rajamani, "High-gain nonlinear observer with lower tuning parameter," *IEEE Trans. Autom. Control*, vol. 64, no. 8, pp. 3194–3209, Aug. 2019.
[34] D. Astolfi, L. Marconi, L. Praly, and A. R. Teel, "Low-power peaking-free high-gain observers," *Automatica*, vol. 98, pp. 169–179, Dec. 2018.

[35] M. Oueder, M. Farza, R. Ben Abdennour, and M. M'Saad, "A high gain observer with updated gain for a class of MIMO non-triangular systems," *Syst. Control Lett.*, vol. 61, no. 2, pp. 298–308, Feb. 2012.

[36] P. Bernard, *Observer Design for Nonlinear Systems*. Springer, 2019.

[37] J. M. Ali, N. H. Hoang, M. A. Hussain, and D. Dochain, "Review and classification of recent observers applied in chemical process systems," *Comput. Chem. Eng.*, vol. 76, pp. 27–41, May 2015.

[38] O. Bernard, G. Sallet, and A. Sciandra, "Nonlinear observers for a class of biological systems: Application to validation of a phytoplanktonic growth model," *IEEE Trans. Autom. Control*, vol. 43, no. 8, pp. 1056–1065, Aug. 1998.

[39] S. I. Biagiola and J. L. Figueroa, "A high gain nonlinear observer: Application to the control of an unstable nonlinear process," *Comput. Chem. Eng.*, vol. 28, no. 9, pp. 1881–1898, Aug. 2004.

[40] F. Lafont, E. Busvelle, and J.-P. Gauthier, "An adaptive high-gain observer for wastewater treatment systems," *J. Process Control*, vol. 21, no. 6, pp. 893–900, Jul. 2011.

[41] A. Rodriguez-Mata, J. Torres-Munoz, A. R. Dominguez, D. Hernandez-Villagran, and S. Celikovsky, "Nonlinear high-gain observers with integral action: Application to bioreactors," in *Proc. 8th Int. Conf. Electr. Eng., Comput. Sci. Autom. Control*, Oct. 2011, pp. 1–6.

[42] A. K. Singh and J. Hahn, "State estimation for high-dimensional chemical processes," *Comput. Chem. Eng.*, vol. 29, nos. 11–12, pp. 2326–2334, Oct. 2005.

[43] S. Nuñez, H. De Battista, F. Garelli, A. Vignoni, and J. Picó, "Second-order sliding mode observer for multiple kinetic rates estimation in bioprocesses," *Control Eng. Pract.*, vol. 21, no. 9, pp. 1259–1265, Sep. 2013.

[44] D. Coutinho, A. Vargas, C. Feudjio, M. Benavides, and A. V. Wouwer, "A robust approach to the design of super-twisting observers–application to monitoring microalgae cultures in photo-bioreactors," *Comput. Chem. Eng.*, vol. 121, pp. 46–56, Feb. 2019.

[45] I. F. Yupanqui Tello, D. Coutinho, J. Winkin, and A. Vande Wouver, "Observer design for chemical tubular reactors based on system linearization," in *Proc. Eur. Control Conf. (ECC)*, May 2020, pp. 1141–1146.

[46] H. J. Sussmann and P. V. Kokotovic, "The peaking phenomenon and the global stabilization of nonlinear systems," *IEEE Trans. Autom. Control*, vol. 36, no. 4, pp. 424–440, Apr. 1991.

[47] A. Levant, "Chattering analysis," *IEEE Trans. Autom. Control*, vol. 55, no. 6, pp. 1380–1389, Jun. 2010.

[48] A. F. Villaverde, "Observability and structural identifiability of nonlinear biological systems," *Complexity*, vol. 2019, Jan. 2019, Art. no. 8497093.

[49] H. K. Khalil, "Cascade high-gain observers in output feedback control," *Automatica*, vol. 80, pp. 110–118, Jun. 2017.

[50] A. M. Gibon-Fargeot, F. Celle-Couenne, and H. Hammouri, "Cascade estimation design for CSTR models," *Comput. Chem. Eng.*, vol. 24, no. 11, pp. 2355–2366, Nov. 2000.

[51] A. J. Whalen, S. N. Brennan, T. D. Sauer, and S. J. Schiff, "Observability and controllability of nonlinear networks: The role of symmetry," *Phys. Rev. X*, vol. 5, no. 1, Jan. 2015, Art. no. 011005.

[52] Y. Y. Liu, J. J. Slotine, and A. L. Barabási, "Observability of complex systems," *Proc. Nat. Acad. Sci. USA*, vol. 110, no. 7, pp. 2460–2465, 2013.

[53] C. Letellier, I. Sendiña-Nadal, and L. A. Aguirre, "Nonlinear graph-based theory for dynamical network observability," *Phys. Rev. E, Stat. Phys. Plasmas Fluids Relat. Interdiscip. Top.*, vol. 98, no. 2, Aug. 2018, Art. no. 020303.

[54] M. R. Mojallizadeh, B. Brogliato, and V. Acary, *Discrete-Time Differentiators: Design and Comparative Analysis*. INRIA, 2020.

[55] M. Ghanes, J.-P. Barbot, L. Fridman, A. Levant, and R. Boisliveau, "A new varying-gain-exponent-based differentiator/observer: An efficient balance between linear and sliding-mode algorithms," *IEEE Trans. Autom. Control*, vol. 65, no. 12, pp. 5407–5414, Dec. 2020.

[56] B. Brogliato, A. Polyakov, and D. Efimov, "The implicit discretization of the supertwisting sliding-mode control algorithm," *IEEE Trans. Autom. Control*, vol. 65, no. 8, pp. 3707–3713, Aug. 2020.

[57] X. Xiong, Z. Liu, S. Kamal, and S. Jin, "Discrete-time super-twisting observer with implicit Euler method," *IEEE Trans. Circuits Syst. II, Exp. Briefs*, vol. 68, no. 4, pp. 1288–1292, Apr. 2021.

[58] S. Yu, X. Yu, B. Shirinzadeh, and Z. Man, "Continuous finite-time control for robotic manipulators with terminal sliding mode," *Automatica*, vol. 41, no. 11, pp. 1957–1964, Nov. 2005.

[59] M. R. Mojallizadeh, B. Brogliato, and V. Acary, "Time-discretizations of differentiators: Design of implicit algorithms and comparative analysis," *Int. J. Robust Nonlinear Control*, vol. 31, no. 16, pp. 7679–7723, 2021.

[60] B. Brogliato and A. Polyakov, "Digital implementation of sliding-mode control via the implicit method: A tutorial," *Int. J. Robust Nonlinear Control*, vol. 31, no. 9, pp. 3528–3586, 2021.

[61] R. Kikuuwe, R. Pasaribu, and G. Byun, "A first-order differentiator with first-order sliding mode filtering," *IFAC-PapersOnLine*, vol. 52, no. 16, pp. 771–776, 2019.

[62] G. Byun and R. Kikuuwe, "An improved sliding mode differentiator combined with sliding mode filter for estimating first and second-order derivatives of noisy signals," *Int. J. Control, Autom. Syst.*, vol. 18, no. 12, pp. 3001–3014, Dec. 2020.

[63] A. F. Villaverde, N. Tsiantis, and J. R. Banga, "Full observability and estimation of unknown inputs, states and parameters of nonlinear biological models," *J. Roy. Soc. Interface*, vol. 16, no. 156, Jul. 2019, Art. no. 20190043.

[64] S. Ding, W. Chen, K. Mei, and D. J. Murray-Smith, "Disturbance observer design for nonlinear systems represented by input–output models," *IEEE Trans. Ind. Electron.*, vol. 67, no. 2, pp. 1222–1232, Feb. 2020.

JOSÉ ANTONIO GONZÁLEZ-PRIETO earned his engineering degree from Universidade de Vigo in Vigo, Spain, in 2005. In 2014, he earned a PhD in control engineering from Universidade de Vigo, Spain. In his current position, he is a teacher at the Centro Universitario de la Defensa (Naval Military School). He is currently interested in sliding mode systems, the analysis of observability of complex systems, the design of high gain observers, the fusion of sensor data, and in the identification of non-linear parameters.

ALEJANDRO F. VILLAVERDE received the M.Eng. degree in electrical engineering and the Ph.D. degree in systems and control engineering from the University of Vigo, Vigo, Galicia, Spain, in 2004 and 2009, respectively. From 2009 to 2015, and from 2016 to 2020, he was a Postdoctoral Researcher with the Bioprocess Engineering Group, IIM-CSIC. From 2015 to 2016, he was an I2C Postdoctoral Fellow with the University of Vigo. He has also carried out stays at the universities of Groningen, MIT, Stanford, Minho, and Oxford. He is currently a Ramón y Cajal Fellow with the Department of Systems Engineering and Control, University of Vigo. His research interests include the identification, analysis, control and optimization of nonlinear systems, with a focus on biological applications. He is also an Academic Editor of *PLOS One* and *Complexity*, and an Associate Section Editor-in-Chief of *Symmetry*.

● ● ●